Simultaneous Attainment of High Electron and Ion Temperatures in Discharges with Internal Transport Barriers in ASDEX Upgrade

S. Günter, R. C. Wolf, F. Leuterer, O. Gruber, M. Kaufmann, K. Lackner, M. Maraschek, P. J. Mc Carthy,* H. Meister, A. Peeters, G. Pereverzev, H. Salzmann, S. Schade, J. Schweinzer, W. Suttrop, and the ASDEX Upgrade Team

Max-Planck-Institut für Plasmaphysik, EURATOM-Association, Garching, Germany

(Received 9 November 1999)

Internal transport barriers have been demonstrated to exist also under conditions with $T_e \approx T_i \approx$ 10 keV and predominant electron heating of the tokamak core region. Central electron cyclotron heating was added to neutral beam injection–heated ASDEX Upgrade discharges with a preexisting internal transport barrier, established through programmed current ramping leading to shear reversal. Compared to a reference internal transport barrier discharge without electron cyclotron resonance heating, the electron heat conductivity in the barrier region was found not to increase, in spite of a fivefold increase in electron heat flux, and also angular momentum and ion energy transport did not deteriorate.

PACS numbers: 52.55.Fa, 52.80.–s

I. Introduction.—The formation of internal transport barriers in discharges with low or reversed central shear has substantially improved the prospects of steady state operation of tokamak fusion reactors [1–6]. The confinement improvement observed reduces the necessary plasma current I_p for high fusion performance (Q = fusion power/externally supplied plasma heating power), the partial access to second stability raises the fraction of I_p provided by the intrinsic bootstrap current, and the bootstrap-driven current density can be arranged to be in reasonable alignment with the one required to maintain the ideal shear profile. Critical issues specific to this operating regime are (1) steady state maintenance of such discharges, (2) the possibility of central impurity accumulation, (3) the extension of the operating regime to higher densities (collisionalities), and (4) its compatibility with predominant electron heating, as provided by thermonuclear α particles. Doubts to the last point arise as the ion temperature gradient (ITG) driven mode, generally considered to dominate discharges with strong additional heating [5], is strongly destabilized by increasing the ratio T_e/T_i. Here we report on the first experiments on ASDEX Upgrade in which electron cyclotron resonance heating (ECRH), applied to a discharge with an existing internal transport barrier (ITB), resulted in high electron temperatures ($T_e \approx T_i \approx 10$ keV), without deteriorating the ion energy transport.

II. Experimental results.—Internal transport barriers are produced by programmed current and heating power ramp-up, leading to low or reversed central shear. The heating method applied is usually neutral beam injection (NBI), which results in efficient electron heating only for $E_{\mathrm{beam}} > 14.8(\mu_{\mathrm{beam}}/\mu_i^{2/3})k_B T_e$ (where E_{beam} is the beam energy, and μ_{beam} and μ_i are the beam and the background ion mass number, respectively). Significant electron heating, at high ion temperatures, has been obtained only in partly ion cyclotron resonance heated discharges on JET [4], in NBI discharges based on negative ion acceleration on JT60-U [7], and in recent combined ECRH-NBI discharges on DIII-D [8]. Although these experiments showed clear barriers also in the electron temperature, they did not attain $T_e \approx T_i$, and they reported a deterioration of ion confinement following the onset of central electron heating [8]. High peak electron temperatures have been achieved in ECRH [9] and lower hybrid [10,11] heated discharges with weak or negative shear in FTU and TORE Supra, albeit at very low ion temperatures, where ITG modes are not expected to play a role. The experiments, reported here, were carried out on the tokamak ASDEX Upgrade ($R_0 = 1.63$ m, $a = 0.5$ m, $b/a = 1.6$) at a toroidal field of $B_t = 2.5$ T, during a current ramp phase ($I_p \approx 1$ MA/s), with plasmas leaning on the high-field sidewall resulting in an L-mode edge. The ECRH system of ASDEX Upgrade allows shot to shot variation of the launch angle of the waves through a poloidally and toroidally movable mirror, so that co- and countercurrent drive, as well as pure heating, is possible, and the power deposition and B_t value can partly be varied independently.

To a reproducible NBI discharge scenario previously established, giving strong ion ITBs in conjunction with an L-mode edge, ECRH power was added in different launch configurations. The corresponding wave forms of I_p, NBI and ECRH heating powers ($P_{\mathrm{NBI}}, P_{\mathrm{ECRH}}$) and line-averaged electron density ($\bar{n}_e$) are shown in Fig. 1. The reference discharge without ECRH power application (Fig. 2a) shows a strongly hollow q profile [according to an equilibrium code reconstruction based on external magnetic signals and ten motional Stark effect (MSE) channels] and an internal barrier formation about 200 ms after application of NBI heating, with ion and electron temperatures reaching 10 and 4 keV, respectively, in the innermost channels accessible to the respective diagnostics (charge exchange recombination spectroscopy and ECE) throughout the whole discharge set.

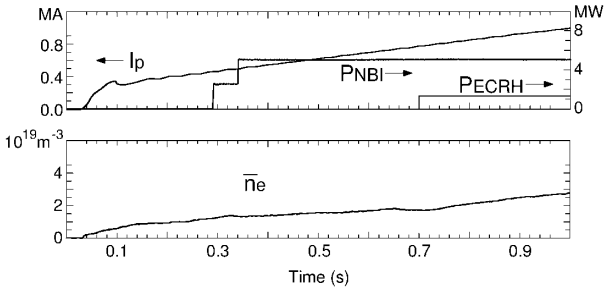

FIG. 1. Typical time evolution of plasma current (I_p), neutral beam heating power (P_{NBI}), and line-averaged density ($\bar{n}_e$) for discharges with strong ion ITBs and L-mode edge. The ECRH power (P_{ECRH}) has been applied with different launch angles allowing for pure heating, co- and countercurrent drive.

An MHD event, discussed below, leads to a temporal breakdown of the ITB at $t = 0.67$ s, when $q_{\min}$, according to the reconstruction, reaches 2. Both T_e and T_i recover, however, thereafter. Central application of electron cyclotron power in countercurrent drive (counter-ECCD; Fig. 2b) or pure heating (ECRH) mirror orientation leads to a rapid, strong increase of T_e, and an approximately 20% further increase in T_i. The electron temperature at the normalized toroidal minor radius $\rho_{\mathrm{tor}} = 0.2$ (the innermost ECE channel useable during ECRH) exceeds 10 keV and is approximately equal to the ion temperature at $\rho_{\mathrm{tor}} = 0.06$. The high electron temperatures and gradients are also confirmed by Thomson scattering. The approximate equivalence between counter-ECCD and pure ECRH discharges was established adjusting, through poloidal orientation of the mirrors, the power deposition profiles. These variations showed also a dependence on the deposition profile in the expected direction (higher T_e for more central deposition). A comparison discharge with cocurrent drive (co-ECCD), on the other hand, does not lead to a recovery of the ITB after the MHD event, but rather a continuous MHD activity, and plasma conditions with $T_e \approx T_i \leq 6$ keV (Fig. 2c).

III. Confinement analysis.—Figures 3 and 4 show measured and derived parameter profiles for the reference discharge (without ECR power) and the counter-ECCD case at $t = 0.97$ s, close to the maximum T_e, T_i for both discharges. The equilibrium reconstruction used for the confinement as well as for the MHD stability analysis is based on the MSE measurements. The radial electric field E_r which has been shown to be important for the analysis of the MSE data [12] is, however, not included since reliable E_r measurements are not available so far. This causes mainly an error of q_0. The value of $q_{\min}$, however, agrees within the error bars, given in Fig. 2, with the appearance of MHD modes as discussed in Sec. IV. The transport coefficients χ_e and χ_i are computed with the ASTRA code [13], run in the interpretative mode with density and temperature profiles fitted to the experimental data. The reference discharge shows a pronounced ITB in T_i and toroidal rotation velocity v_{tor}, and a weak one in T_e, located just inside the $q = q_{\min}$ radius. The NBI energy deposition is peaked at the center, with only a small fraction of the power ($\geq$10%) going into the electrons. The resulting profiles of heat conductivity coefficients (Fig. 3d) show $\chi_e < \chi_i$ with the latter, in the barrier region, being close to the neoclassical value. With counter-ECCD (or pure ECRH) applied, the electron heat flux dominates the ion one within the $\rho_{\mathrm{tor}} = 0.2$ surface, the electron transport barrier becomes prominent, the electron temperature inside the barrier zone more than doubles, and also the central ion temperature increases slightly. Contrary to the observation on DIII-D, the central plasmas rotation velocity does not decrease [8].

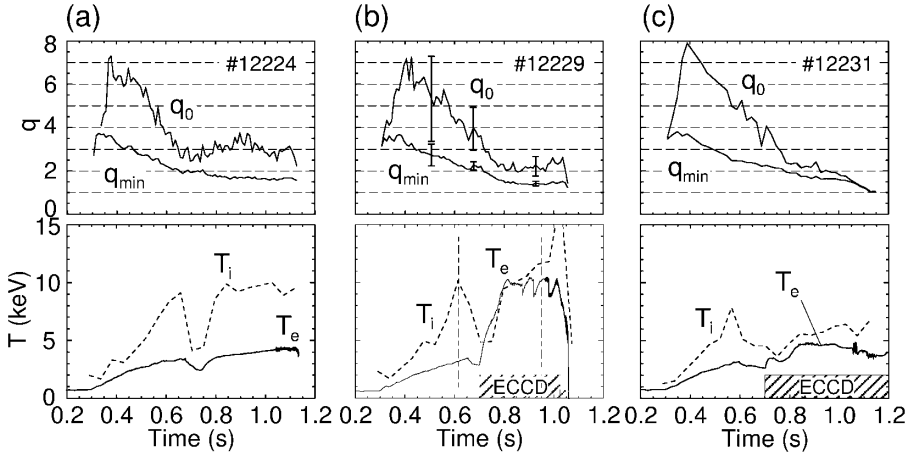

FIG. 2. Comparison of three types of discharges: (a) the reference case with NBI heating only, (b) NBI and counter-EC current drive, and (c) NBI and co-ECCD. Shown are the time evolution of the central and the minimum q value, and the maximum values of ion and electron temperature obtained from charge exchange recombination and electron cyclotron emission (ECE), respectively. Whereas the ion temperature is measured at $\rho_{\mathrm{tor}} = 0.06$, due to the central ECRH deposition the innermost ECE channel is located at $\rho_{\mathrm{tor}} = 0.2$. The time resolution of the ECE measurement is very high ($\Delta t = 1$ ms); the ion temperature, however, is measured only every 65 ms. In (b) the time points for the profiles given in Figs. 3 and 4 are indicated by vertical lines.

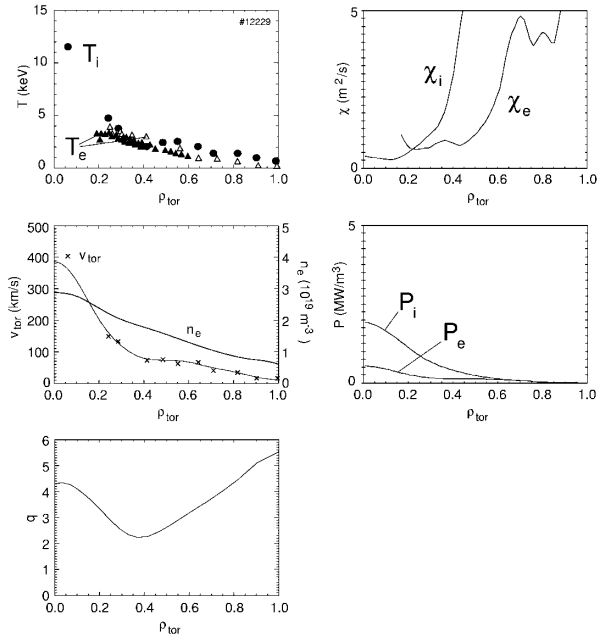

FIG. 3. Profiles of the electron, T_e (△), measured by ECE and Thomson scattering, respectively, and the ion temperature, T_i (•), the ion (χ_i) and electron (χ_e) heat conductivities, electron density (n_e), toroidal rotation velocity ($v_{\rm tor}$), electron and ion heating power deposition (P), and the q profile for the discharge shown in Fig. 2b (#12229) at $t = 0.62$ s.

In spite of the fivefold increase in electron heat flux, the electron heat conductivity in the barrier region does not increase but shows even indications of a decrease. The ion heat conductivity remains approximately invariant,

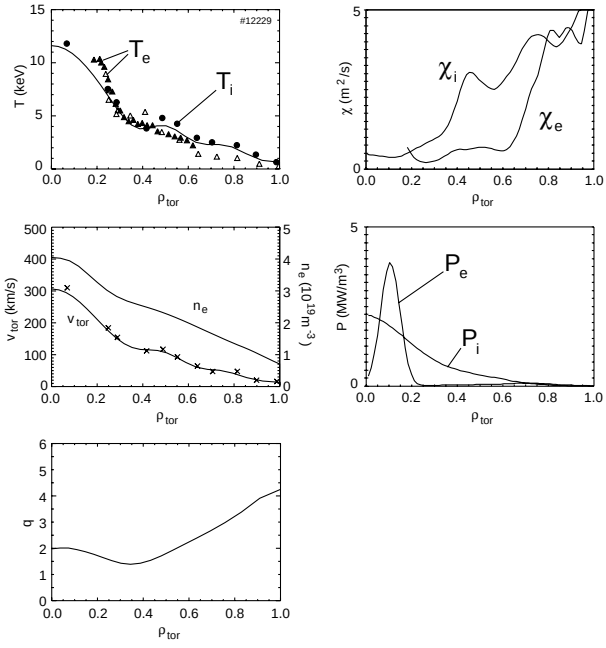

FIG. 4. The same profiles as in Fig. 3 for discharge #12229 at a later time ($t = 0.95$ s).

with the slight T_i increase as a result of the reduced collisional energy transfer from thermal and beam ions to the electrons.

IV. Influence of MHD modes.—The behavior of these discharges is obviously strongly affected by MHD activity. The temporal breakdown of the internal transport barrier visible in Fig. 2 has been described for the reference discharge conditions (without EC power application) in Ref. [14], and is due to a saturated double tearing mode, clamping temporarily also the q profile at $q_{\rm min} = 2$. This mode arises if $q_{\rm min}$ slightly drops below 2, and disappears either following the drop of $q_{\rm min}$ well below 2 (due to the decoupling of the two rational surfaces with rising distance and differential rotation) or the increase of central electron temperature following ECRH or counter-ECCD. A tentative explanation for the latter observation could be the increased pressure gradient at the inner $q = 2$ surface, giving rise—in inversion of the dynamics leading to the neoclassical tearing modes in positive shear regions—to a stabilization of the mode due to the combined effect of bootstrap current reduction in the island and of the negative magnetic shear. For the counter-ECCD case of Fig. 2b, a stability analysis with the CASTOR code, again based on measured q and pressure profiles shows the fast T_e crashes occurring later in the discharge to be caused by infernal modes, which are probably also responsible for the ultimate disruptive end of this and the other discharges. In the co-ECCD case, the $(m, n) = (2, 1)$ double tearing mode is followed by $(2, 1)$ and $(3, 1)$ MHD activity with tearing-type parity (as determined by comparison of the ECE signals with CASTOR eigenfunctions), evidently caused by the local drop in central q. Such a strong effect on stability would be consistent with estimates of the current profile changes induced by ECCD given by TORAY (combined electron cyclotron wave and Fokker-Planck electron dynamics) and ASTRA (current diffusion) code calculations, which predict for this case a change of the core plasma current of 90 kA, located inside $\rho_{\rm tor} = 0.2$, 500 ms after the onset of ECCD, corresponding to the measured decrease of q_0 by $\Delta q_0 = 1.5$.

V. Summary.—The above experiments have clearly established that strong internal transport barriers are well compatible with the reactor-relevant conditions of predominant electron heating and $T_e \approx T_i$, provided MHD-stable corridors in parameter space can be identified and followed. Future experiments will aim at a better control of MHD activity, utilizing, in addition to ECCD also the 6 MW Fast-Wave Current Drive system becoming available on ASDEX Upgrade in 2000.

*University College Cork, Association EURATOM-DCU, Cork, Ireland.

[1] F. M. Levinton *et al.*, Phys. Rev. Lett. **75**, 4417 (1995).
[2] B. W. Rice *et al.*, Phys. Plasmas **3**, 1983 (1996).

[3] T. Fujita *et al.,* Phys. Rev. Lett. **78**, 2377 (1997).
[4] F. X. Söldner *et al.,* Nucl. Fusion **39**, 407 (1999).
[5] O. Gruber *et al.,* Phys. Rev. Lett. **83**, 1787 (1999).
[6] R. E. Waltz *et al.,* Phys. Plasmas **4**, 2482 (1997).
[7] Y. Kamada and the JT-60 Team, Plasma Phys. Controlled Fusion **41**, B77 (1999).
[8] B. W. Stallard *et al.,* Phys. Plasmas **6**, 1978 (1999).
[9] P. Buratti *et al.,* Phys. Rev. Lett. **82**, 560 (1999).
[10] X. Litaudon *et al.,* Plasma Phys. Controlled Fusion **38**, 1603 (1996).
[11] A. A. Tucillo *et al.,* in *Radio Frequency Power in Plasma,* edited by R. M. Ryan and T. Intrator, AIP Conf. Proc. No. 403 (AIP, New York, 1997), p. 121.
[12] B. W. Rice *et al.,* Phys. Rev. Lett. **79**, 2694 (1994).
[13] G. Pereverzev *et al.,* "ASTRA An Automatic System for Transport Analysis in a Tokamak," IPP Report No. IPP 5/42, 1991.
[14] S. Günter *et al.,* Plasma Phys. Controlled Fusion **41**, B231 (1999).